

# Load Frequency Control in Two Area Power Systems in A Smart Grid Environment

Faradji Mohamed  
dept. University of M'Hamed Bougara  
Boumerdes  
Laboratory of Systems Engineering and  
Telecommunications  
Boumerdes, Algeria  
m.faradji@univ-boumerdes.dz

Toufik Madani Layadi  
dept. University of Mohamed El Bachir  
El Ibrahimi  
Laboratory of Materials and Electronic  
Systems  
Bordj Bou Arreridj, Algeria  
toufikmadani.layadi@univ-bba.dz

Ilhami Colak  
Department of Electrical and  
Electronics Engineering, Istinye  
University  
Istanbul, Turkiye  
ilhcol@gmail.com

**Abstract**—Load Frequency Control (LFC) is a critical aspect of power system stability, ensuring that the frequency and tie-line power flow remains within acceptable limits. In this paper, we investigate LFC in a two-area system with the integration of demand response (DR) loops. The DR loops allow for dynamic adjustments of load demand based on real-time system conditions. Our study focuses on optimizing the proportional-integral-derivative (PID) controller used in the LFC system. To achieve this, we perform a comparative analysis of three optimization algorithms: Artificial bee colony (ABC), particle swarm optimization (PSO), and Aquila Optimization (AO). These algorithms are applied to tune the PID controller parameters, aiming to enhance system performance, reduce frequency deviations, and minimize control efforts. Simulation results demonstrate the effectiveness of the proposed approach. The optimized PID controller, combined with DR, significantly improves system response during load disturbances. Furthermore, the comparative study sheds light on the strengths and weaknesses of each optimization algorithm, providing valuable insights for future LFC implementations. Overall, our work contributes to the advancement of LFC strategies in interconnected power systems, emphasizing the role of demand response and optimization techniques in achieving robust and efficient control

**Keywords**— Load Frequency Control, demand response, style, optimization algorithms, proportional-integral-derivative

## I. INTRODUCTION

Load frequency control is essential in the design of electrical power systems, having long been a key aspect of power system operations. It aims to achieve two main goals: keeping the system's frequency deviation within specific limits and managing tie-line power interchange deviations. The core concepts of load frequency control are well-documented in [1-5]. Typically classified as a secondary-level control, load frequency control is crucial in automatic generation control (AGC), a feedback system that continuously adjusts generator output to maintain a predefined system frequency. In multi-area interconnected power systems, load frequency control (LFC) is vital for achieving generator load control, eliminating steady-state frequency errors, and optimizing transient behavior [6]. Over the years, LFC has become integral to automatic generation control strategies in electric power systems, with the conventional proportional-integral (PI) controller being widely used among the various types of load frequency controllers. While PI, PID, Fuzzy-PID, and ANFIS controllers offer simplicity in implementation and

provide satisfactory dynamic responses, their performance can deteriorate when the system faces complexities, such as load variations. Hence, there is a growing need for controllers who can effectively address these challenges. This study evaluates the performance of three optimization algorithms—Artificial Bee Colony (ABC), Particle Swarm Optimization (PSO), and Aquila Optimization—in improving the efficiency of a Proportional-Integral-Derivative (PID) controller for load frequency control (LFC). The two areas studied experience different load variations and generation imbalances. Our comparative analysis examines the effects of these optimization methods on LFC performance, considering both scenarios with and without demand response mechanisms. By including demand response, we factor in the dynamic behavior of consumers and their readiness to modify consumption patterns based on price signals or grid conditions.

## II. LOAD FREQUENCY CONTROL

In a power system where numerous loads are connected, the speed and frequency naturally fluctuate in response to governor characteristics and load variations. If there's no need to maintain a constant frequency, there's typically no requirement to adjust the generator settings.[9] However, when a constant frequency is necessary, the wind turbine speed can be modified by adjusting the governor's characteristics. Consider a scenario where two generating stations are interconnected via a tie line. If load variations occur at either end, and the goal is to maintain a constant frequency, this is referred to as Flat Frequency Regulation.

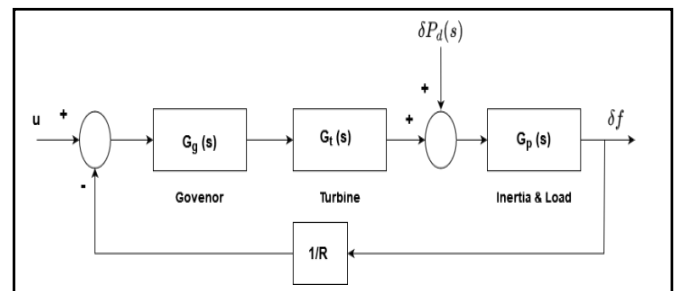


Fig. 1. Linear model of a single-area power system

There are three main scenarios to consider:

- Flat Frequency Regulation: In this case, both areas (A and B) strive to maintain a constant frequency.
- Parallel Frequency Regulation: Here, both areas (A and B) must maintain a constant frequency simultaneously.
- Flat Tie-line Loading Control: This involves frequency maintenance within a specific area using its generators while also ensuring constant tie-line loading.

In Selective Frequency Control, each system autonomously manages load variations within its limits without impacting the maintenance of other systems in the group.

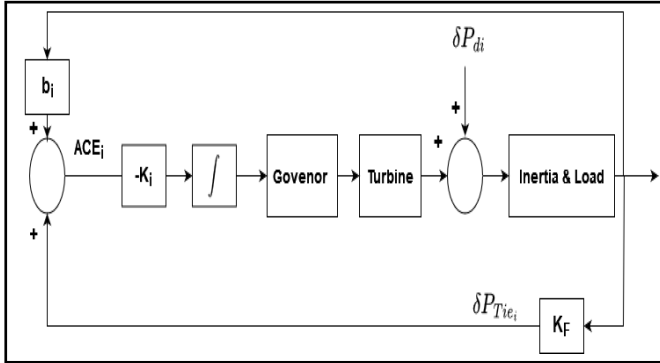


Fig. 2. Frequency control system using conventional control

On the other hand, Tie-line Load-Bias Control involves collaboration among all interconnected systems to maintain frequency, regardless of where load variations occur. It typically includes a primary load frequency controller and a tie-line plotter to determine the input power on the tie for precise frequency control. To regulate the system frequency, each area is equipped with PID controllers.

### III. DEMAND RESPONSE

Smart grids operate more efficiently with the implementation of demand-response (DR) strategies [6]. These strategies are pivotal in managing electricity usage, especially during peak times, to enhance the grid's reliability. DR itself is multifaceted, with various types encompassing distinct advantages and challenges. We can broadly classify DR into three primary categories. The first category focuses on reducing electricity consumption through two main types of programs: time-based and incentive-based. Time-based programs, also known as price-based programs, offer consumers dynamic pricing set by the utility company, reflecting the cost of energy at different times. Incentive-based programs, on the other hand, involve fixed or dynamic payments to consumers who lower their power use during peak hours, with penalties for non-compliance [7]. The second category includes task-scheduling and energy-management DR systems, also referred to as energy-scheduling DR methods. Task scheduling allows consumers to choose when to activate their charge, shifting it away from peak demand periods. Energy management strategies adjust the power consumption of specific loads to reduce overall demand during peak times [8].

Lastly, DR methods are categorized based on the communication model into centralized and distributed

systems. In centralized systems, the energy utility makes load activation or scheduling decisions based on consumer data. Each consumer individually contributes to the overall solution. Centralized systems are employed for scheduling and controlling appliances, buildings, PHEV charging stations, and DR applications in microgrids. Conversely, distributed systems rely on collaborative efforts among consumers to lessen the overall load, guided by prices from the utility that reflect the total system load. This approach promotes scalability and protects consumer privacy by avoiding centralized data collection for decision-making [9].

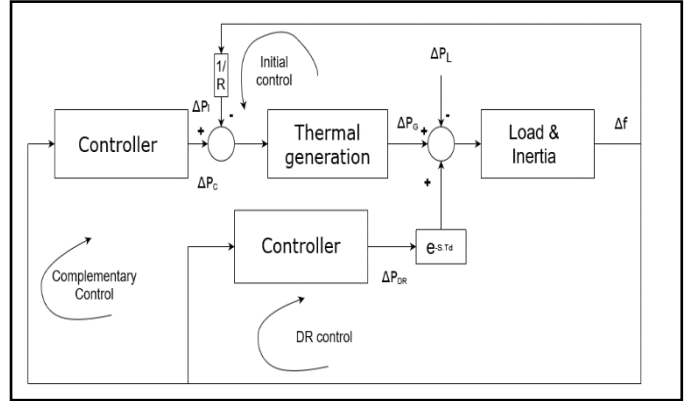


Fig. 3. A depiction of a single-area power system

The general low-order linearized power system model for frequency control synthesis and analysis is described by the power balance equation in the frequency domain.

$\Delta P_G(s) - \Delta P_L(s)$  : incremental power mismatch;

$\Delta f(s)$  : frequency deviation;

$2M$  : equivalent inertia constant;

$LD$  : equivalent load-damping coefficient;

$s$  : Laplace transform operator.

This model is essential for understanding and managing the frequency stability of power systems, which is crucial for maintaining the balance between power generation and consumption.

$$\Delta P_G(s) - \Delta P_L(s) = 2M \cdot s \cdot \Delta f(s) + LD \cdot \Delta f(s) \quad (1)$$

Since Demand Response (DR) for Ancillary Services (AS) functions similarly to spinning reserves, it plays a vital role in stabilizing the power system. Spinning reserves are backup power resources that can be quickly activated to compensate for power imbalances. Similarly, DR involves adjusting the power consumption of certain loads to balance supply and demand. When the system frequency deviates from its nominal value, a negative frequency deviation (indicating a power deficit) necessitates turning off a portion of responsive loads (DR) to reduce demand. Conversely, a positive frequency deviation (indicating a power surplus) requires turning on additional loads to increase demand. By integrating DR into the power balance equation, we can modify the equation as follows:

$$\Delta P_G(s) - \Delta P_L(s) + \Delta P_{DR}(s) = 2M \cdot s \cdot \Delta f(s) + LD \cdot \Delta f(s). \quad (2)$$

Here,  $\Delta P_G(s)$  represents the change in generation power,  $\Delta P_L(s)$  represents the change in load power, and  $\Delta P_{DR}(s)$  represents the change in power due to DR. The term  $2M \cdot s \cdot \Delta f(s)$  accounts for the inertial response of the system,

where  $M$  is the inertia constant and  $s$  is the Laplace transform variable. The term  $LD \cdot \Delta f(s)$  represents the damping effect, where  $LD$  is the load-damping coefficient.

Our model considers that the effect of DR is separated from the inherent load-damping parameter. Load damping is a natural property of the system, reflecting how the load inherently responds to frequency changes, while DR is an intentional and controllable action implemented to manage the system frequency. By separating these effects, we can design a more realistic control strategy.

Additionally, the modified equation allows for a distinct control loop for DR. This separation not only improves the accuracy of the model but also enhances the structure for controller design. Having a dedicated control loop for DR enables more precise and flexible control of the power system. The parameters of the system can represent the equivalent characteristics of all generation assets and load damping within the same area. This single-area model is selected to convey the main idea of this paper. However, in future work, we plan to extend this model to multi-area interconnected power systems. These larger systems involve multiple generation companies (Gencos) and load aggregators (Lagcos), which will require more complex modeling and control strategies.

Unlike traditional spinning reserve-provider power plants, DR resources do not have ramp-up or ramp-down limitations. This means that the power consumption status of controllable loads can be changed instantaneously based on the command signals they receive. The primary constraint for DR is communication delay (latency), which can impact the dynamic performance of the system. Efficient communication systems are crucial to ensure that DR actions are implemented quickly and accurately to maintain system stability.

#### IV. SIMULATION MODEL

This article explores a modified two-area power system, used as a test model, where each area has a generation capacity of 2500 MW. The system is designed to represent modern power grids and includes various components and constraints to reflect real-world conditions. Each area in the system features a conventional thermal power generating unit. These units are subject to several physical constraints that affect their operation:

- **Governor Dead Band (GDB):** This is a small range around the set point where changes in frequency do not cause the governor to respond. It helps in preventing unnecessary adjustments for minor frequency deviations.
- **Generation Rate Constraints (GRC):** These constraints limit the rate at which power output can change. In this model, the GRC is set at 3% per minute, or 0.0005 per second, meaning the power output can only increase or decrease by this amount within the specified time frame.
- **Boiler Dynamics:** These describe the behavior and response time of the boiler in the thermal power plant, which affects how quickly the plant can adjust its output.

- **Solar Photovoltaic (SPV) System:** This represents the integration of solar power generation, which contributes to the overall power capacity and can influence the system's frequency response.
- **Wind Turbine (WT):** This includes the wind power generation component, adding variability and renewable energy sources to the system.
- **Demand Response (DR) Regulation Loop:** This is a mechanism where consumers adjust their power usage in response to supply conditions, helping to balance demand and supply.

The Generation Rate Constraints (GRC) are particularly important as they ensure that the power output changes gradually, which is crucial for maintaining system stability and avoiding sudden disruptions. Figure 3 in the article illustrates the generalized model of the proposed frequency response system, which incorporates the Demand Response (DR) mechanism. This model demonstrates how various components work together to maintain the frequency stability of the power system despite changes in demand and supply. The objective of the frequency control scheme is to ensure that each control area can meet its own energy needs while simultaneously maintaining compatibility with frequency control measures.

##### A. Wind Turbine Generator Modeling

The power output of a wind turbine is directly influenced by the speed of the wind. Wind speed comprises several components: base speed ( $S_{WB}$ ), gust speed ( $S_{WG}$ ), ramp speed ( $S_{WR}$ ), and noise speed ( $S_{WN}$ ) of wind. Therefore, the total wind speed ( $S_w$ ) can be expressed as:

$$S_w = S_{WB} + S_{WG} + S_{WR} + S_{WN}. \quad (3)$$

To model the basic properties of wind, which include base fluctuations and randomness, a simplified version of wind speed can be represented as:

$$S_w = S_{WB} + S_{WN}. \quad (4)$$

The base wind component  $S_{WB}$  is a constant value that is present when the wind turbine generator is operational. The randomness of  $S_{WB}$  can be described using the Heaviside step function:

$$S_{WB} = C = 7.5 H(t) + 4.5 H(t - 10) - 2.5 H(t - 15). \quad (5)$$

where  $H(t)$  is the Heaviside step function.

The noise component ( $S_{WN}$ ) of the wind speed can be expressed using a complex formula:

$$S_{WN} = 2 \sigma^2 \sum_{i=0}^N \sqrt{Sv(\omega i) \Delta \omega \cos(\omega i t + \Phi i)}. \quad (6)$$

where  $\omega i = \left(i - \frac{1}{2}\right) \Delta$ ,  $\Phi i$  is a random variable with a uniform probability density in the range  $[0, 2\pi]$ ,  $\Delta \omega$  ranges from 0.5 to 2 radians per second,  $\sigma^2$  is the variance of the noise component (set to 200),  $Sv(\omega i)$  is the spectral density function, and  $N = 50$ . The spectral density function  $SV(\omega i)$  is given by:

$$SV(\omega i) = \frac{2L_N F^2 |\omega i|}{(\pi^2 [1 + (\frac{F \omega i}{\mu \pi})^2]^{\frac{4}{3}})}. \quad (7)$$

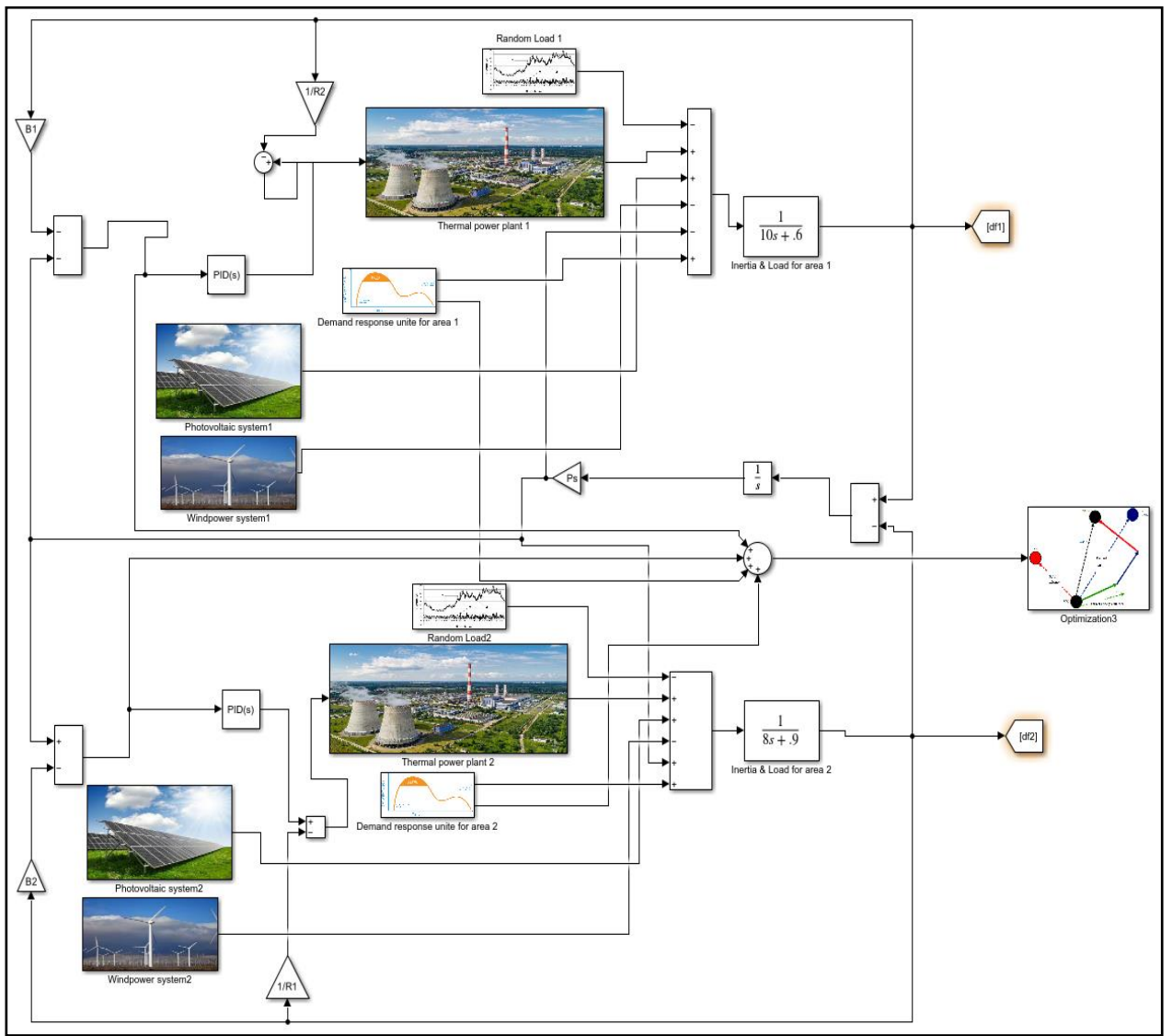


Fig. 4. Simulink model in for two area frequency control system with DR loops.

Where,  $L_N$  is the surface drag coefficient (0.04),  $F$  is the length scale of turbulence (2000 meters), and  $\mu$  is the mean wind speed (7.5 m/s). The power generated by the wind turbine ( $P_w$ ) can be calculated from the wind speed ( $V_w$ ) using the following equation [14]:

$$P_w = \frac{1}{2} \rho B C_{o_p} V_w^3. \quad (8)$$

Where,  $\rho$  is the air density (1.25 kg/m<sup>3</sup>), and  $B$  is the swept area of the turbine blades (1735 m<sup>2</sup>).  $B C_{o_p}$  is the power coefficient calculated as:

$$C_p = (0.44 - 0.0167\beta) \sin \left[ \frac{(\lambda - 3)}{15 - 0.3\beta} \right] - 0.0184(\lambda - 3)\beta. \quad (9)$$

Here,  $\lambda$  is the tip speed ratio, given by  $\lambda = \frac{R_{blade} \omega_{blade}}{V_w}$ , and  $R_{blade}$  is the length of the turbine blades (23.5 meters),  $\omega_{blade}$  is the rotational speed of the blades (3.1428 radians per second), and  $\beta$  is the blade pitch angle (0.1745 radians).

A detailed description of considered WTG is given in [21]. The transfer function of WTG is represented by linear first-order lag as [21]

$$G_{WTG}(s) = \frac{K_{WTG}}{1+sT_{WTG}} = \frac{P_{WTG}}{P_w} \quad (10)$$

where  $K_{WTG} = 1$ , is the gain constant and  $T_{WTG} = 1.5$  is the time constant. In this model, all nonlinearities are neglected for simplicity.

## B. Modeling of Solar Photovoltaic (SPV) System

The power output of the solar photovoltaic (SPV) system, measured in watts, can be determined using the following formula[14]:

$$P_{Pv} = \eta S \varphi \{1 - 0.005(T_a + 25)\} \quad (11)$$

Here,  $\eta$  is the conversion efficiency of the SPV cell, set at 10%,  $S$  is the area of the SPV array, which is 4084 square meters;  $\varphi$  is the input solar irradiation, measured in kilowatts per square meter (kW/m<sup>2</sup>). and  $T_a$  is the atmospheric temperature, which is 25°C in this context. In this formula  $P_{Pv}$  is the power output of the SPV system. The term  $(1 - 0.005(T_a + 25))$  accounts for the efficiency loss due to temperature. As the temperature increases, the efficiency of the SPV cells decreases slightly. The power output  $P_{Pv}$  is directly proportional to the solar irradiation  $\varphi$ . This means that as the solar irradiation increases, the power output also increases. Solar radiation ( $\varphi$ ) is expressed using the Heaviside step function, which represents sudden changes in solar radiation over time. The equation for ( $\varphi$ ) is:

$\varphi = 0.52H(t) - 0.032H(t - 10) + 0.079H(t - 20) + \varphi_n(t)$  where  $H(t)$  is the Heaviside step function.  $\varphi_n(t)$  is the stochastic (random) component of solar radiation, which varies within the range of -0.1-0.1-0.1 to 0.10.10.1 kW/m<sup>2</sup>. The transfer function of the SPV system, which describes how the output responds to changes in input over time, is represented by a linear first-order lag model:

$$G_{SPV}(s) = \frac{K_{SPV}}{1+sT_{SPV}} \quad (12)$$

where  $K_{SPV} = 1$  is the gain constant, indicating a direct proportionality between input and output, and  $T_{SPV} = 1.8$  s the time constant, which describes how quickly the SPV system responds to changes in solar irradiation. In this model, all nonlinearities are neglected to simplify the analysis, meaning the response is assumed to be linear.

## V. RESULTS AND DISCUSSION

Integrating a Solar Photovoltaic (SPV) system and a Wind Turbine (WT) into a microgrid introduces significant variability in power generation, which presents a challenge to the stability of frequency regulation. To address this, a Load Frequency Control (LFC) mechanism utilizing a Proportional-Integral-Derivative (PID) controller and DR loop has been developed [12][13]. This hybrid control strategy is designed to take the frequency error and its rate of change as inputs, which are then processed to optimize the PID controller parameters using three distinct optimization algorithms.

The effectiveness of this approach is evident from the data presented in Figures 5 through 8. These figures illustrate that the (DR) loop, when integrated with PID-based control, markedly improves the dynamic response of the microgrid system compared to traditional control methods. Notably, the DR loop significantly reduces both the maximum overshoot in frequency and the time required for the system to stabilize at a steady state.

Upon comparing the three optimization algorithms, it is observed that the (PSO) algorithm outperforms the others in terms of achieving a rapid steady state and minimizing the maximum overshoot. This indicates that PSO is highly effective in fine-tuning the PID controller parameters for optimal frequency regulation within the microgrid. The (ABC) algorithm also shows considerable improvement when used in conjunction with the DR loop. It demonstrates a substantial reduction in both the maximum overshoot and the

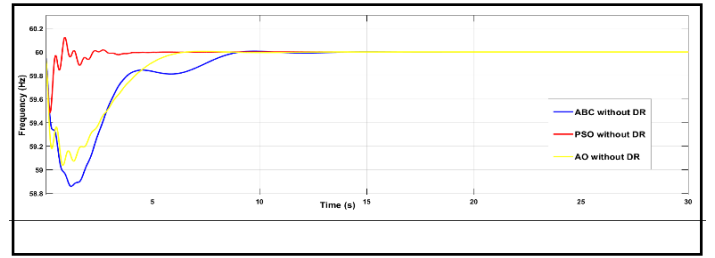


Fig.7. freq. deviation of Area-2 with Demand response control

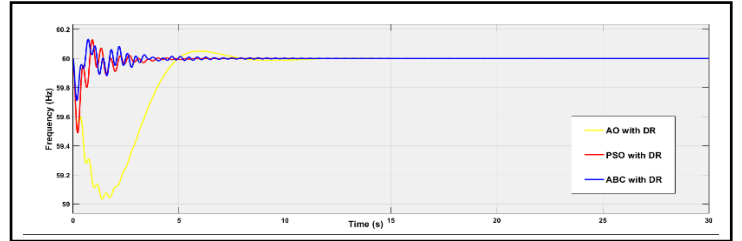


Fig.8. freq. deviation of Area-2 without Demand response

Time taken to reach a steady frequency state, suggesting that ABC is a viable option for optimizing PID controller settings in this context.

However, the (AO) algorithm, despite showing some improvement with the DR loop, does not yield results that are consistent or reliable enough to be considered a dependable optimization method for this specific case study. The AO algorithm's performance indicates that while it may contribute to some extent, it lacks the robustness and reliability required for effective frequency regulation in a microgrid environment.

The integration of SPV and WT systems into a microgrid necessitates advanced LFC strategies. The hybrid PID controller, optimized by PSO and ABC algorithms, demonstrates superior performance in maintaining frequency stability. These findings underscore the potential of advanced optimization techniques in enhancing the dynamic response and reliability of microgrids with high penetration of renewable energy sources."

## VI. CONCLUSION

This study investigates a two-area system in a smart grid environment with a DR loop with PID controller optimized with PSO ABC and AO optimization algorithms for frequency regulation. The findings underscore the critical influence of DR in diminishing the maximum overshoot and accelerating the attainment of a steady-state frequency. Among the tested algorithms, PSO emerged as the superior optimizer for PID controller adjustments in frequency regulation. Its rapid convergence, straightforward operation, robust performance, and high-quality optimization outcomes distinctly outperform its counterparts. These attributes render PSO exceptionally compatible with the dynamic and intricate demands of power system frequency control, confirming its suitability for complex, real-world applications in smart grid management.

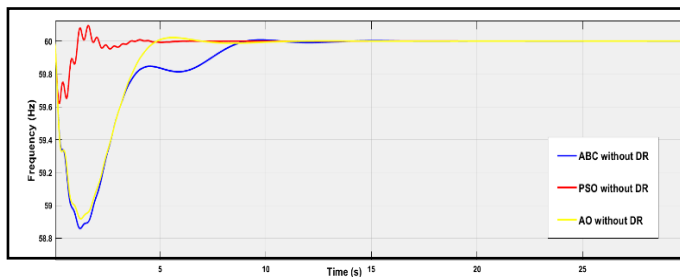


Fig. 5. freq. deviation of Area-1 without Demand response control

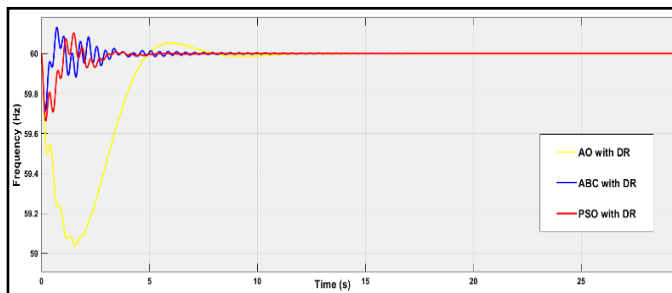


Fig. 6. freq. deviation of Area-1 with Demand response control

## REFERENCES

- [1] Satish Kumar Meena, Saurabh Chanana, Comparative Study Of Load Frequency Control Using PID and FGPI Controller, IEEE power India International Conference, pp.1-6 (2014)
- [2] K. Sabahi M.A. Nekoui M. Teshnehlab M. Aliyari M. Mansouri Load frequency control in interconnected power system using modified dynamic neural networks” proceeding of the 15th Mediterranean conference on control and amp; Automation pp. T26-011 (2007).
- [3] Hadi Saadat “power System Analysis” in McGraw Hill (2002)..
- [4] Manoj Kumar Debnath, Ranjan Kumar Mallick, Sadhana Das, Aditya Aman “Gravitational Search Algorithm (GSA) Optimized Fuzzy-PID Controller Design for Load Frequency Control of an Interconnected Multi-Area Power System” International Conference on Circuit, Power and Computing Technologies, pp.1-6 (2016) .
- [5] Hauk Gozde M. Cengiz Taplamacioglu Ilhan Kocaarslan, Comparative performance analysis of Artificial Bee Colony algorithm in automatic generation control for interconnected reheat thermal power system, International Journal of Electrical Power and amp; Engergy Systems vol.42 no.1 pp.167- 178 (2012).
- [6] Gharbi, A., Ayari, M., & Yahya, A. E. (2023). Demand-Response Control in Smart Grids. *Applied Sciences (Switzerland)*, 13(4). <https://doi.org/10.3390/app13042355>
- [7] Lu, R.; Hong, S.H. Incentive-based demand response for smart grid with reinforcement learning and deep neural network. *Appl. Energy* 2019, 236, 937–949. <https://doi.org/10.1016/j.apenergy.2018.12.061>
- [8] Javanmard, B.; Tabrizian, M.; Ansarian, M.; Ahmarinejad, A. Energy management of multi-microgrids based on game theory approach in the presence of demand response programs, energy storage systems and renewable energy resources. *J. Energy Storage* 2021, 42, 102971.. <https://doi.org/10.1016/j.est.2021.102971>
- [9] Pi, Z.; Li, X.; Ding, Y.; Zhao, M.; Liu, Z. Demand response scheduling algorithm of the economic energy consumption in buildings for considering comfortable working time and user target price. *Energy Build.* 2021, 250, 111252 <https://doi.org/10.1016/j.enbuild.2021.111252>
- [10] Shahbazitabar, M., Abdi, H., Nourianfar, H., Anvari-Moghaddam, A., Mohammadi-Ivatloo, B., Hatziargyriou, N. (2021). An Introduction to Microgrids, Concepts, Definition, and Classifications. In: Anvari-Moghaddam, A., Abdi, H., Mohammadi-Ivatloo, B., Hatziargyriou, N. (eds) *Microgrids. Power Systems.* Springer, Cham. [https://doi.org/10.1007/978-3-030-59750-4\\_1](https://doi.org/10.1007/978-3-030-59750-4_1)
- [11] Gaddameedhi, S., Gaddameedhi, S., Vidya Sagar, E., Susheela, N., & Gaddamedhi, S. (2024). *INTERNATIONAL JOURNAL OF RENEWABLE ENERGY RESEARCH Performance Investigation of PV Battery Integrated Parallel Operated Inverters in Standalone Mode* (Vol. 14, Issue 1).
- [12] Patel, D., Bhongade, S., Singh, A., & Mandloi, R. S. (2024). *Optimizing Load Frequency Control in Power Systems: A Comparative Study of BWOA and PSO-Tuned PID Controllers* (Vol. 8, Issue 1).
- [13] Bouhouta, A., Moulahoum, S., Kabache, N., Moualdia, A., & Colak, I. (n.d.). *Harmonics Compensation of Grid-Connected PV Systems Using a Novel M5P Model Tree Control*.
- [14] Ren, H., Zhang, H., Deng, G., & Hou, B. (2018). Feedforward Feedback Pitch Control for Wind Turbine Based on Feedback Linearization with Sliding Mode and Fuzzy PID Algorithm. *Mathematical Problems in Engineering*, 2018. <https://doi.org/10.1155/2018/4606780>